Stellar Dynamics and Star Formation Histories of z ~ 1 Radio-loud Galaxies

Barišić, Ivana; van der Wel, Arjen; Bezanson, Rachel; Pacifici, Camilla; Noeske, Kai; Muñoz-Mateos, Juan C.; Franx, Marijn; Smolčić, Vernesa; Bell, Eric F.; Brammer, Gabriel; ...

Stellar Dynamics and Star Formation Histories of $z \sim 1$ Radio-loud Galaxies

Ivana Barišić[1] [iD], Arjen van der Wel[1] [iD], Rachel Bezanson[2] [iD], Camilla Pacifici[3] [iD], Kai Noeske[4], Juan C. Muñoz-Mateos[5],
Marijn Franx[6] [iD], Vernesa Smolčić[7], Eric F. Bell[8] [iD], Gabriel Brammer[9] [iD], João Calhau[10], Priscilla Chauké[1] [iD],
Pieter G. van Dokkum[11] [iD], Josha van Houdt[1], Anna Gallazzi[12] [iD], Ivo Labbé[6] [iD], Michael V. Maseda[6] [iD], Adam Muzzin[13] [iD],
David Sobral[6,10] [iD], Caroline Straatman[1] [iD], and Po-Feng Wu[1]

[1] Max-Planck Institut für Astronomie, Königstuhl 17, D-69117, Heidelberg, Germany; barisic@mpia.de
[2] Department of Astrophysics, Princeton University, Princeton, NJ 08544, USA
[3] Astrophysics Science Division, Goddard Space Flight Center, Code 665, Greenbelt, MD 20771, USA
[4] experimenta gGmbH, Kranenstraße 14, 74072 Heilbronn, Germany
[5] European Southern Observatory, Alonso de Córdova 3107, Casilla 19001, Vitacura, Santiago, Chile
[6] Leiden Observatory, Leiden University, P.O. Box 9513, NL-2300 AA Leiden, The Netherlands
[7] Department of Physics, Faculty of Science, University of Zagreb, Bijenicka cesta 32, 10000 Zagreb, Croatia
[8] Department of Astronomy, University of Michigan, 1085 S. University Avenue, Ann Arbor, MI 48109, USA
[9] Space Telescope Science Institute, 3700 San Martin Drive, Baltimore, MD 21218, USA
[10] Department of Physics, Lancaster University, Lancaster LA1 4 YB, UK
[11] Department of Astronomy, Yale University, New Haven, CT 06511, USA
[12] INAF-Osservatorio Astrofsico di Arcetri, Largo Enrico Fermi 5, I-50125 Firenze, Italy
[13] Department of Physics and Astronomy, York University, 4700 Keele Street, Toronto, Ontario, ON MJ3 1P3, Canada
Received 2017 June 1; revised 2017 August 2; accepted 2017 August 11; published 2017 September 21

Abstract

We investigate the stellar kinematics and stellar populations of 58 radio-loud galaxies of intermediate luminosities ($L_{3\,\text{GHz}} > 10^{23}\,\text{W Hz}^{-1}$) at $0.6 < z < 1$. This sample is constructed by cross-matching galaxies from the deep VLT/VIMOS LEGA-C spectroscopic survey with the VLA 3 GHz data set. The LEGA-C continuum spectra reveal for the first time stellar velocity dispersions and age indicators of $z \sim 1$ radio galaxies. We find that $z \sim 1$ radio-loud active galactic nucleus (AGN) occur exclusively in predominantly old galaxies with high velocity dispersions: $\sigma_* > 175\,\text{km s}^{-1}$, corresponding to black hole masses in excess of $10^8\,M_\odot$. Furthermore, we confirm that at a fixed stellar mass the fraction of radio-loud AGN at $z \sim 1$ is five to 10 times higher than in the local universe, suggesting that quiescent, massive galaxies at $z \sim 1$ switch on as radio AGN on average once every Gyr. Our results strengthen the existing evidence for a link between high black hole masses, radio loudness, and quiescence at $z \sim 1$.

Key words: galaxies: evolution – galaxies: fundamental parameters – galaxies: high-redshift – galaxies: jets – galaxies: star formation

1. Introduction

To match the stellar and dark matter halo mass functions and reproduce their evolution through cosmic time, semi-analytical and hydrodynamical galaxy formation models rely on two primary feedback channels to decrease the efficiency of star formation. These models implement heating by supernovae that lead to a low star formation efficiency in low-mass dark matter halos (White & Rees 1978; White & Frenk 1991; Hopkins et al. 2012). Feedback from super-massive black holes (SMBHs) is implemented to prevent excessive star formation in high-mass halos (Bower et al. 2006; Croton et al. 2006; De Lucia & Blaizot 2007; Vogelsberger et al. 2014; Schaye et al. 2015). The physical prescriptions differentiate between radiative-mode feedback and jet-mode feedback. Radiative-mode feedback (quasar mode) is associated with the high accretion rate of the cold gas onto the SMBH and is related to the gas outflows (Shakura & Sunyaev 1973; Di Matteo et al. 2005). Jet-mode (radio mode) feedback is associated with a low accretion rate of hot ("coronal") gas onto the SMBH. The feedback loop is thought to exist between the cooling of hot gas that feeds the SMBH (e.g., Blanton et al. 2001) to trigger an active galactic nuclei (AGNs) phase that subsequently provides a heating source, counter-acting cooling and preventing further growth in stellar mass.

Direct observational evidence for a link between AGNs and the heating of halo gas is found in massive clusters, where radio jets are seen to produce cavities in the X-ray emitting gas (see McNamara & Nulsen 2007; Heckman & Best 2014, and references therein) and also in early-type galaxies in lower-mass groups where the presence of cold gas and radio jets is linked to the thermodynamical state of the warm/hot gas (Werner et al. 2012, 2014). Furthermore, indirect evidence in the form of a strong correlation between a lack of star formation (quiescence) and the presence of radio AGNs has been gathered for galaxies in the local universe (e.g., Matthews et al. 1964; Kauffmann et al. 2003a; Best et al. 2005). This correlation suggests that massive galaxies spend extended periods in a radio-loud AGN phase, which provides sufficient energy to keep the halo gas from cooling.

Until recently, radio observations of high-redshift galaxies were limited to the very highest luminosities ($L > 10^{24}\,\text{W Hz}^{-1}$), where radio AGN hosts are the most extreme galaxies: the brightest cluster galaxies, but also star-bursting galaxies (De Breuck et al. 2002; Willott et al. 2003). Deep surveys with the Karl G. Jansky Very Large Array (VLA) are now probing lower luminosities ($L \gtrsim 10^{22}\,\text{W Hz}^{-1}$), enabling us to explore the link between radio AGNs and quiescence at large look-back time. Donoso et al. (2009) showed that the fraction of radio-loud galaxies increases out to $z \sim 1$ and that its power-law dependence on stellar mass ($f_{\text{radio-loud}} \propto M_*^{2.5}$) is consistent with what is seen for present-day galaxies (Best et al. 2005). Simpson et al. (2013) demonstrate that up to $z \sim 1$ radio AGN preferentially reside in galaxies with evolved stellar populations as traced by the
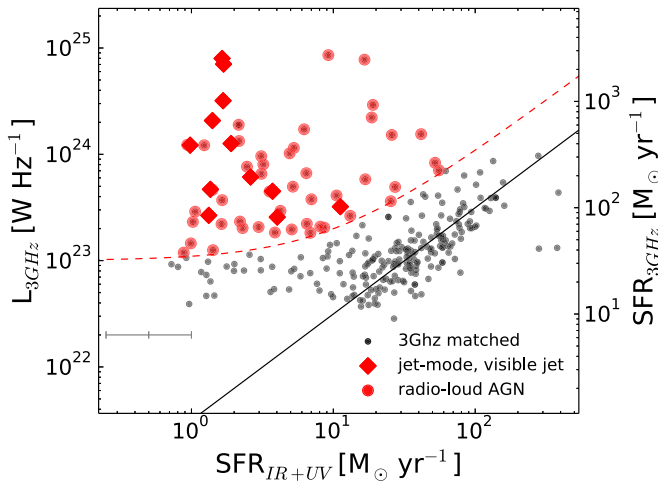
Figure 1. The 3 GHz radio luminosity (left-hand y-axis) and implied SFR (right-hand y-axis) vs. SFR_{UV+IR} for the LEGA-C+VLA cross-matched sample. The red points meet our luminosity criteria for radio-loud AGNs, and the red diamonds have visible jets in the radio image. The gray error bar represents the typical uncertainty of the SFR_{UV+IR}. The 3 GHz luminosity uncertainties for radio-loud AGN are smaller than the size of the data points.

Figure 2. Classification of galaxies on jet-mode/radiative-mode based on the ratio of optical emission lines [O III]/Hβ and [O II]/Hβ (see Section 2.4 for details).

$D_n(4000)$ index. Rees et al. (2016) confirm these results, but show that at $z > 1$ radio AGNs are hosted more frequently by star-forming galaxies. Finally, Williams and Röttgering (2015) demonstrate that the fraction of radio-loud AGNs of luminosities $>10^{24}\,\mathrm{W\,Hz^{-1}}$ increases out to $z = 2$, that the power-law mass dependence becomes flatter with the increasing mass, and that the slope of mass dependence becomes shallower with the increasing redshift.

In this study, we use deep, rest-frame optical spectra from the Large Early Galaxy Astrophysics Census (LEGA-C) survey of galaxies in the redshift range $0.6 < z < 1$ (van der Wel et al. 2016). The LEGA-C optical spectra provide us, for the first time, with direct constraints on recent and long-term star formation histories and stellar dynamical properties of a large sample of galaxies at large look-back time. Cross-matching the LEGA-C sample with the recently completed 3 GHz VLA survey (Smolcic et al. 2017) allows us to examine for the first time stellar populations and velocity dispersions of intermediate luminosity radio-loud AGN at these redshifts. The aim of this paper is to test the hypothesis that radio-loud AGNs preferably occur in quiescent galaxies with large velocity dispersions (black hole masses) over a broad range in cosmic time. The confirmation of this hitherto poorly constrained assumption is crucial for the radio-mode feedback picture.

This paper is organized as follows. In Section 2, we give an overview of LEGA-C and VLA data sets, and introduce the selection criteria and classification scheme for the radio-loud sub-sample. We present our main results and describe stellar content and star formation activity of radio-loud AGN in Section 3. Finally, we summarize our work in Section 4.

2. Data, Sample Selection and Classification

In this section, we give an overview of the data sets analyzed in this work. We present the criteria adopted for the selection of the radio-loud sub-sample among the whole LEGA-C sample, and we describe the method used to classify the radio-loud galaxies into quiescent and star-forming galaxies. By comparing
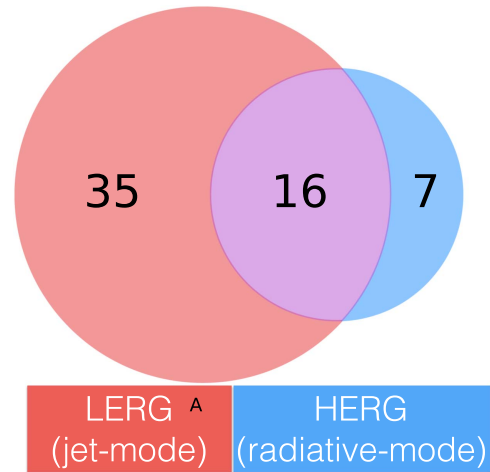
with local benchmark samples, we also measure the evolution of the fraction of radio-loud galaxies out to $z \sim 1$.

2.1. LEGA-C

The LEGA-C survey (van der Wel et al. 2016) is an ESO public spectroscopic survey with VLT/VIMOS (LeFevre et al. 2003) with the aim of obtaining high signal-to-noise ratio $(\mathrm{S/N} \sim 20\,\text{\AA}^{-1})$ continuum spectra of $0.6 < z < 1$ galaxies. The full LEGA-C sample will consist of more than 3000 galaxies, K-band selected from the Muzzin et al. (2013) UltraVISTA survey in the 1.62 square degree region within the COSMOS field (Scoville et al. 2007). The spectral resolution is $R = 2500$, spanning the wavelength range from 6300 Å to 8800 Å. The current paper uses the Data Release II[14] sample of 1989 galaxies observed during the first two years of LEGA-C observations. This sample is representative of the final one, which in turn is representative of the galaxy population at a given K-band flux density. That is, our sample selection is independent of galaxy color and morphology.

In this study, we use redshifts; stellar velocity dispersions; $D_n(4000)$ break and Hδ absorption indices; nebular emission line equivalent widths, as well as physical parameters estimated from broad-band photometry (UV+IR star formation rates (SFR) and stellar masses). UV and IR luminosity based SFRs are estimated following Whitaker et al. (2012). Stellar masses are derived by using an initial mass function (Chabrier 2003), dust extinction (Calzetti et al. 2000), and stellar population libraries and exponentially declining SFR (Bruzual & Charlot 2003). For further details on the data reduction steps and the method used to derive the physical parameters, see van der Wel et al. (2016).

2.2. VLA–COSMOS

We use the observations at 3 GHz (10 cm) (PI: Vernesa Smolčić) covering the 2 square degree COSMOS field, obtained by the VLA radio interferometer. The observations were conducted between 2012 and 2014 with a total observation time of 384 hours, yielding a final mosaic with

---

Table 1
Physical Properties of the Observed Sub-sample of Radio-loud Galaxies

ID	R.A.	Decl.	$z_{\rm spec}$	$L_{3\,\rm GHz}$ [W Hz^{-1}] $\cdot 10^{23}$	$\alpha_3^{1.4{\rm a}}$	d [kpc][b]	Flag[c]
126578	150.09805	2.281367	0.750	2.89 ± 0.18	-0.46 ± 0.14	$\cdots$	1
140050	150.14168	2.446062	0.899	8.04 ± 0.42	-0.03 ± 0.11	$\cdots$	0.5
209637	150.10378	2.507702	0.608	3.21 ± 0.17	-0.93 ± 0.19	17.69 ± 5.10	0
131063	150.35016	2.334642	0.667	12.27 ± 0.63	-0.41 ± 0.09	$\cdots$	1
182797	150.39577	2.481532	0.903	2.22 ± 0.17	<-0.42	$\cdots$	1
184916	150.42589	2.513884	0.679	6.11 ± 0.33	<1.77	50.00 ± 5.36	1
185625	150.42506	2.524558	0.984	1.83 ± 0.18	<-0.89	$\cdots$	0.5
210716	150.17261	2.523343	0.69	12.21 ± 0.60	-0.80 ± 0.08	$\cdots$	1
106926	150.29488	2.034494	0.955	77.68 ± 3.91	1.02 ± 0.09	$\cdots$	0.5
108227	150.26643	2.049850	0.960	7.07 ± 0.39	-0.41 ± 0.31	$\cdots$	0.5
109352	150.10892	2.063952	0.724	4.96 ± 0.28	$-0.49^{+0.16}_{-0.17}$	$\cdots$	1
110509	150.26849	2.077003	0.667	6.64 ± 0.34	-0.06 ± 0.14	$\cdots$	1
110805	150.17149	2.084074	0.729	3.77 ± 0.20	$-0.82^{+0.16}_{-0.17}$	$\cdots$	0.5
113394	150.35657	2.117532	0.875	2.02 ± 0.16	<-0.48	$\cdots$	1
128311	150.05669	2.301382	0.730	4.49 ± 0.24	-0.50 ± 0.28	19.12 ± 5.52	1
129746	150.02608	2.318864	0.941	3.40 ± 0.24	<0.13	$\cdots$	0.5
205180	150.00731	2.453467	0.730	18.94 ± 0.96	$-0.43^{+0.07}_{-0.08}$	$\cdots$	1
209377	150.02267	2.508070	0.746	85.76 ± 4.47	-0.79 ± 0.07	$\cdots$	0
210031	150.02242	2.516584	0.679	5.82 ± 0.29	-0.93 ± 0.13	$\cdots$	0
210739	150.00941	2.526713	0.733	4.09 ± 0.24	-0.49 ± 0.25	$\cdots$	1
234067	149.85017	2.452237	0.714	29.15 ± 1.48	-0.35 ± 0.07	$\cdots$	1
236682	149.87180	2.479084	0.734	20.77 ± 1.04	-0.78 ± 0.07	95.81 ± 5.53	1
236994	149.86151	2.484360	0.730	2.57 ± 0.16	-0.65 ± 0.29	109.57 ± 5.52	1
129631	149.98328	2.317157	0.934	9.60 ± 0.49	-0.61 ± 0.16	$\cdots$	0.5
131657	149.95264	2.341849	0.945	2.33 ± 0.19	-1.06 ± 0.20	$\cdots$	1
169076	149.78040	2.318275	0.677	1.96 ± 0.12	-0.43 ± 0.17	$\cdots$	1
169901	149.79379	2.327209	0.893	2.64 ± 0.19	<-0.23	$\cdots$	0
210564	149.91573	2.521326	0.729	6.55 ± 0.35	-0.47 ± 0.14	$\cdots$	1
235394	149.76112	2.460729	0.671	4.92 ± 0.25	$0.09^{+0.28}_{-0.29}$	$\cdots$	1
235431	149.78880	2.466439	0.732	1.19 ± 0.11	<-0.61	$\cdots$	0.5
237437	149.79221	2.489063	0.734	1.25 ± 0.11	<-0.56	$\cdots$	1
111543	149.91492	2.094372	0.884	2.09 ± 0.17	<-0.54	$\cdots$	0.5
113852	150.01424	2.123182	0.675	31.92 ± 1.59	-0.47 ± 0.07	35.63 ± 5.34	1
125257	150.06847	2.265479	0.979	3.62 ± 0.25	<-0.04	$\cdots$	0.5
147270	149.87502	2.062635	0.847	12.63 ± 0.65	-1.28 ± 0.07	51.16 ± 5.81	1
151161	149.89481	2.109374	0.666	7.65 ± 0.43	-0.004 ± 0.14	$\cdots$	1
161004	149.83919	2.226176	0.943	4.68 ± 0.28	-0.82 ± 0.32	24.00 ± 6.00	0.5
105328	149.90935	2.013062	0.848	1.84 ± 0.15	<-0.45	$\cdots$	1
117992	149.94199	2.173145	0.688	2.31 ± 0.14	-0.28 ± 0.32	$\cdots$	1
120120	149.99265	2.202235	0.629	2.21 ± 0.13	$-0.59^{+0.27}_{-0.25}$	$\cdots$	1
157229	149.74300	2.179562	0.631	15.21 ± 0.75	-0.64 ± 0.08	$\cdots$	0.5
212718	150.07712	2.548955	0.890	70.58 ± 0.62	<-1.03	247.90 ± 5.84	1
203666	150.39935	2.794159	0.822	8.33 ± 0.43	-0.95 ± 0.19	$\cdots$	0.5
215835	150.24612	2.585822	0.675	10.21 ± 0.53	0.34 ± 0.15		0.5
217020	150.16193	2.601267	0.893	2.07 ± 0.18	<-0.55	$\cdots$	1
218725	150.04684	2.620396	0.736	2.94 ± 0.18	-1.03 ± 0.11	$\cdots$	0
232020	150.01646	2.784381	0.983	15.48 ± 0.78	-0.69 ± 0.17	$\cdots$	0.5
232196	149.98419	2.787762	0.853	4.63 ± 0.28	-0.96 ± 0.33	$\cdots$	0.5
245325	149.88518	2.581121	0.694	4.47 ± 0.24	-0.13 ± 0.11	$\cdots$	1
94215	150.68156	2.324819	0.978	2.04 ± 0.20	<-0.81	$\cdots$	0
94982	150.63631	2.333361	0.609	11.47 ± 0.63	-0.32 ± 0.09	$\cdots$	1
96860	150.66121	2.364529	0.826	79.72 ± 0.52	<-1.03	150.99 ± 5.77	1
182890	150.61380	2.484840	0.744	1.45 ± 0.11	<-0.41	$\cdots$	1
183927	150.61508	2.500369	0.796	2.66 ± 0.17	<0.26	458.54 ± 5.69	1
225672	149.91795	2.701692	0.892	17.19 ± 0.85	-0.75 ± 0.1	$\cdots$	0
233281	149.94615	2.801806	0.611	12.19 ± 0.61	-1.20 ± 0.23	59.58 ± 5.11	1
250117	149.77776	2.645909	0.737	22.20 ± 1.12	-0.52 ± 0.08	$\cdots$	0.5
27265	150.14487	1.776603	0.733	13.33 ± 0.39	<2.21	$\cdots$	1

Notes.
[a] Radio spectral slope α inferred using $S \propto \nu^\alpha$ at 1.4 GHz and 3 GHz.
[b] Linear size (diameter) of the jet, with the errors estimated from the beam size ($0\rlap{.}''75$).
[c] Classification of galaxies onto LERG (1) or HERG (0). For conflicting indicators, we classify galaxies as 50% LERG (0.5).
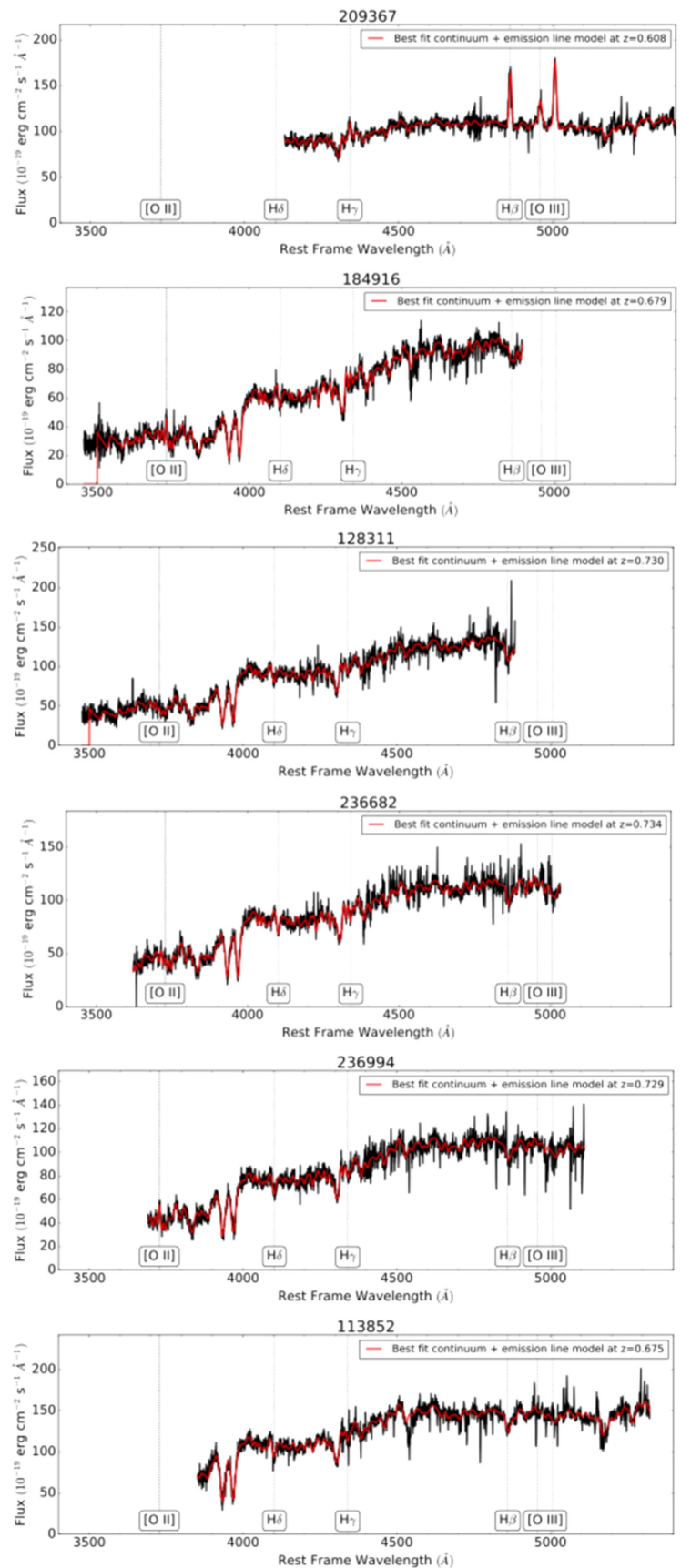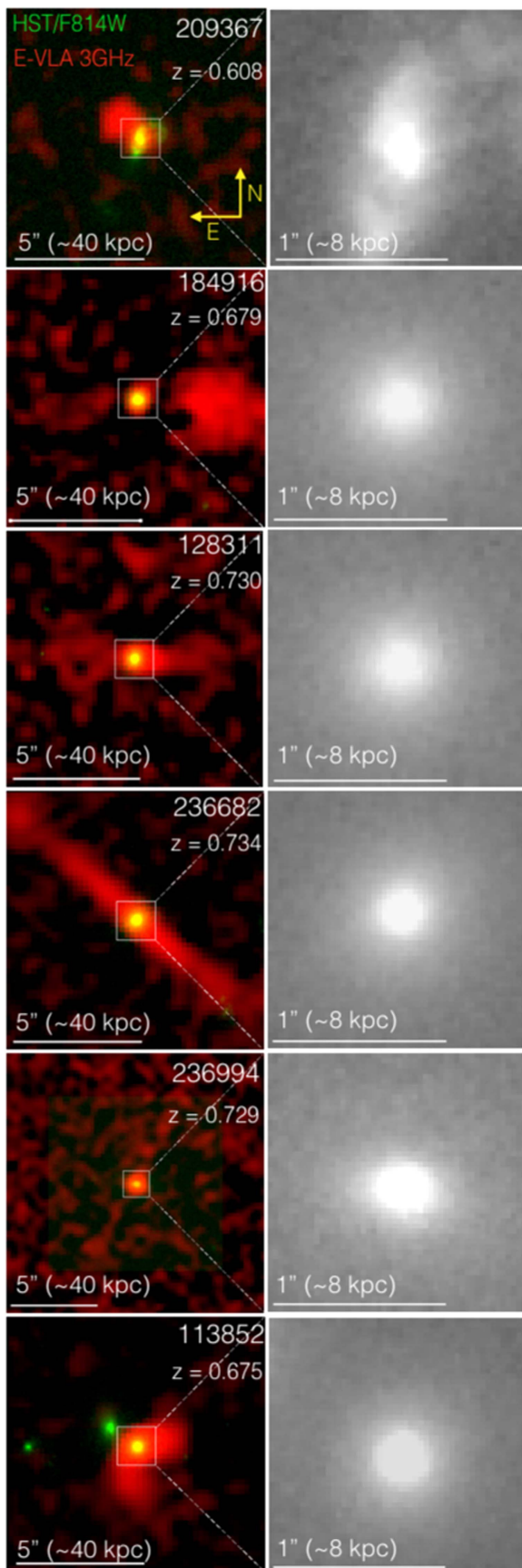
Figure 3. False-color *HST*/ACS/F814W+VLA/3 GHz images of radio sources with visible jets in the 3 GHz data, along with the corresponding LEGA-C optical spectra (black) with the best-fitting stellar continuum model (red).
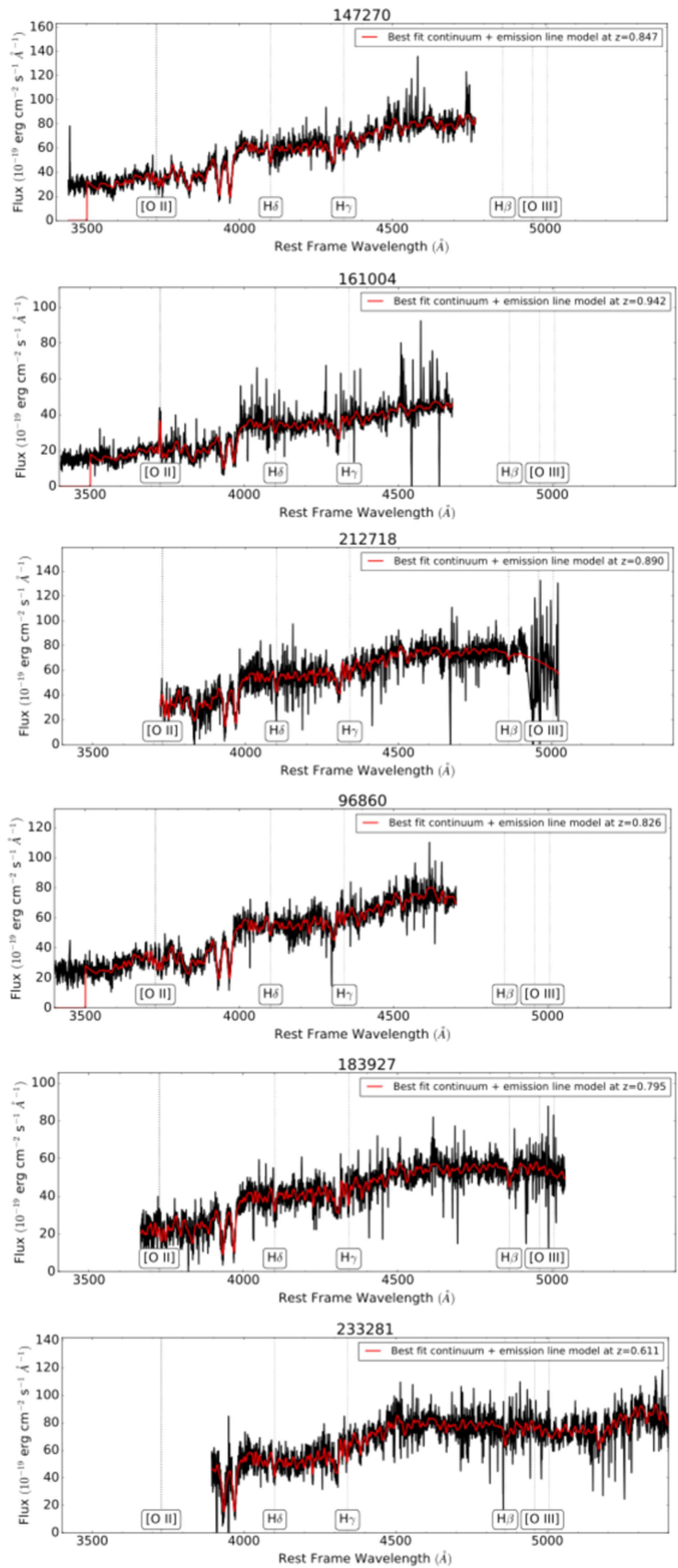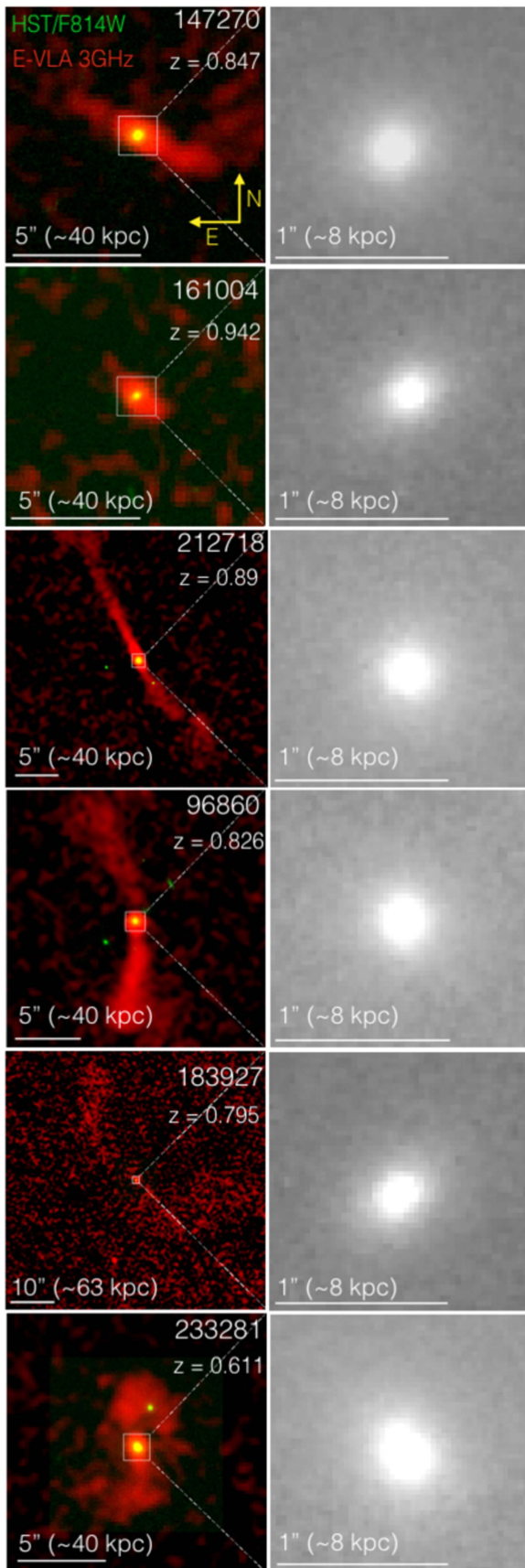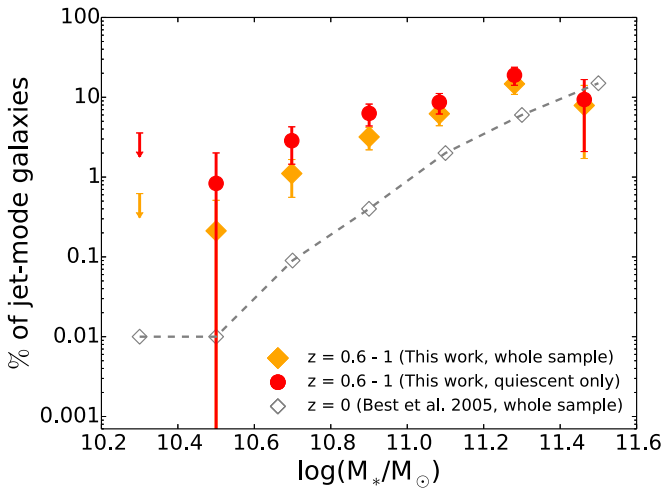
Figure 3. (Continued.)

Figure 4. Fraction of jet-mode galaxies among all and quiescent galaxies in the LEGA-C as a function of the stellar mass (orange diamonds and red circles, respectively). The open orange diamonds show the fraction of jet-mode galaxies for the sample of present-day galaxies.

the angular resolution of $0\overset{''}{.}75$ and a median rms of $2.3\,\mu$Jy beam^{-1}. For further details, see Smolcic et al. (2017).

2.3. Selection of Radio-loud AGN

The current LEGA-C data set contains 1989 galaxies, out of which 322 are found to have a radio counterpart after cross-matching the LEGA-C survey catalog and the VLA 3 GHz 5.5σ catalog (Smolcic et al. 2017). The matching radius between LEGA-C and VLA coordinates is $0\overset{''}{.}7$. The systematic offset in right ascension and declination is $0\overset{''}{.}1$ and $0\overset{''}{.}03$ respectively, while the random offset is $0\overset{''}{.}1$. We convert radio continuum fluxes for cross-matched sources to luminosities, using VLA 3 GHz flux densities and LEGA-C spectroscopic redshifts, following the Condon (1992) luminosity relation. Implied radio-based star formation rates are then found from luminosities using Bell (2003) calibration of the radio-FIR correlation.

Figure 1 compares the radio luminosity, L_{3GHz} (and the corresponding star formation rate) with the UV+IR-based SFR for this cross-matched sample. The good correspondence between the star formation rate indicators is by construction, as the radio-based SFR is calibrated with the SFR derived from the IR luminosity. We see no evidence for a change in the far-infrared to radio luminosity ratio q, but this is not inconsistent with the evidence for such evolution (Magnelli et al. 2015; Delhaize et al. 2017) obtained from larger samples across a much larger redshift range than $z = 0$ to $z = 1$.

Of interest for this study are the sources that are outliers from the one-to-one relation (black line); that is, the sources with excessive radio luminosities. We estimate the radio AGN luminosity by subtracting three times the radio luminosity expected on the basis of the UV+IR-based SFR from the observed radio luminosity. That is, we allow for a factor 3 scatter in the radio-SFR relation. Adopting the radio luminosity limit from Best et al. (2005), we select those 58 galaxies with radio AGN luminosities $>10^{23}$ W Hz^{-1} as our radio-loud AGN sample (see Figure 1, red dashed curve).

2.4. Classification of the Radio-loud Objects

We examine the optical spectra of the 58 radio-loud AGNs to distinguish between jet-mode (low-excitation radio galaxy, LERG) and radiative-mode (high-excitation radio galaxy, HERG) based on the presence or absence of strong high-excitation emission lines (Hine & Longair 1979; Laing 1994). We classify a radio galaxy as a LERG if there are no or only low-excitation (Balmer) emission lines (EW([O III], [O II], [Hβ]) > -5 Å). For systems with strong emission lines, we classify those with high [O III]λ5007/Hβ and/or [O II]λ3727/Hβ ratios (>1) as HERGs. In our sample of 58 radio-loud AGNs, 35 are classified as LERGs and seven as HERG with high confidence. The classification of 16 objects remains undetermined, as we were not able to discriminate with high confidence between jet/radiative-mode. For the remainder of this paper, we consider these objects as LERGs with 50% probability for the purpose of statistical calculations. In Figure 2, we summarize the results of our classification, which illustrates that almost 60% of our sample are LERGs. We list the properties of the 58 radio AGNs in Table 1.

We examine the VLA 3 GHz images of our sample for visual confirmation of radio jets. Forty-six radio-loud galaxies are consistent with point sources, but in 12 cases we identify extended morphologies. We show the VLA 3 GHz and *Hubble Space Telescope (HST)* F814W images, as well as the LEGA-C spectra of these 12 objects, in Figure 3.

3. Properties of $z \sim 1$ Jet-mode Galaxies

3.1. Fraction of Jet-mode Galaxies

Using the selection criteria defined in Section 2.4, we determine the fraction of jet-mode radio galaxies in the LEGA-C sample, considering both star-forming and quiescent galaxies (see Figure 4). Because we adopt the radio-loud AGN selection criteria from Best et al. (2005), we compare our fraction of jet-mode galaxies at a redshift range $0.6 < z < 1$ with their fraction of jet-mode galaxies for present-day galaxies. At fixed mass, the fraction of jet-mode galaxies is on average five to 10 times higher at $0.6 < z < 1$ when compared with the present-day universe. Furthermore, we notice the flattening of the power-law mass dependence for the highest mass bin. These findings are consistent with the measurements from Donoso et al. (2009).

One possible evolutionary scenario is that galaxies grow in stellar mass by a factor of two from $z \sim 1$ to the present, while conserving the fraction of jet-mode galaxies. This would imply that growth in stellar mass exceeds growth in black hole mass if we assume that the black hole mass is the only factor that sets the probability or frequency of becoming a radio galaxy. Alternatively, if BHs and stellar mass grow in lockstep (e.g., Calhau et al. 2017), then more frequent (or longer) radio-loud AGN phases at fixed BH mass could be understood by shorter cooling times at earlier cosmic times. The evolution in the fraction of jet-mode AGN in quiescent galaxies must be even faster than that of the general population, given that the fraction of quiescent galaxies is lower at $z \sim 1$ than at the present day (e.g., Bell et al. 2004; Faber et al. 2007). We show the fraction of jet-mode AGN in quiescent galaxies in Figure 4, and see that above $10^{11}\,M_{\odot}$ the fraction of jet-mode galaxies reaches 20%.

The fraction of jet-mode AGNs also strongly depends on stellar velocity dispersion σ_*, which can be seen as a proxy for black hole mass. In Figure 5, we show that more than $\sim$10% of
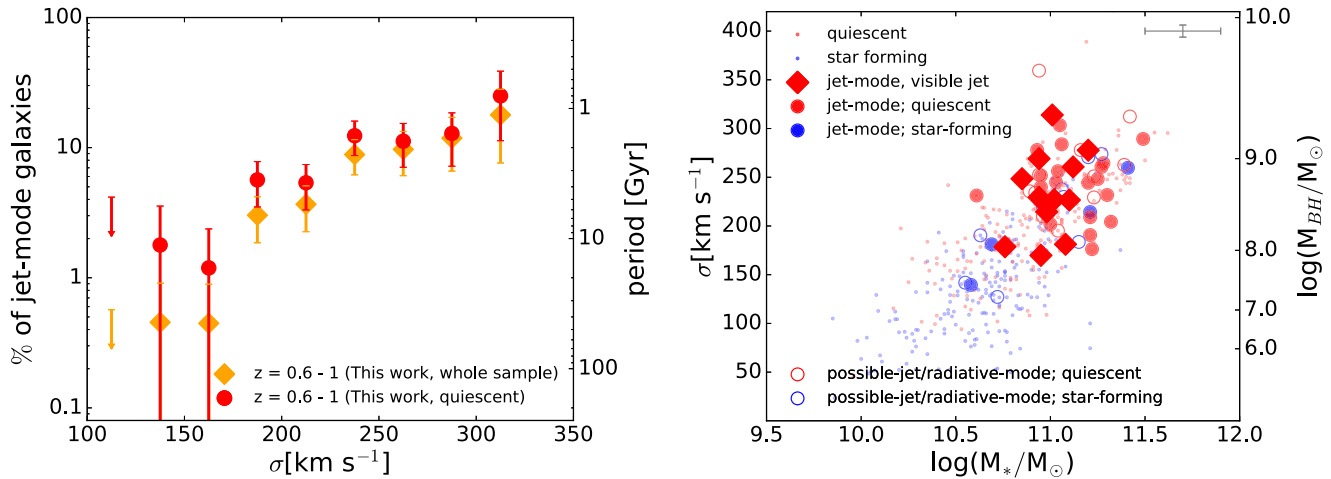
Figure 5. Left: fraction of jet-mode galaxies among the full LEGA-C sample (orange diamonds) and among the quiescent galaxies the LEGA-C sample (red diamonds) as a function of the stellar velocity dispersion σ_*, Right: stellar velocity dispersion σ_* as a function of the stellar mass. The blue and red points mark star-forming and quiescent galaxies, respectively. Large symbols represent radio AGNs, with the filled symbols showing those that are securely classified as jet-mode/low-excitation AGNs (see Section 2.4). Large diamonds represent those with visible jets in the radio image (see Figure 3). Jet-mode AGNs occur in massive galaxies with high stellar velocity dispersions, and old stellar populations. Typical error bars are indicated in the corners.
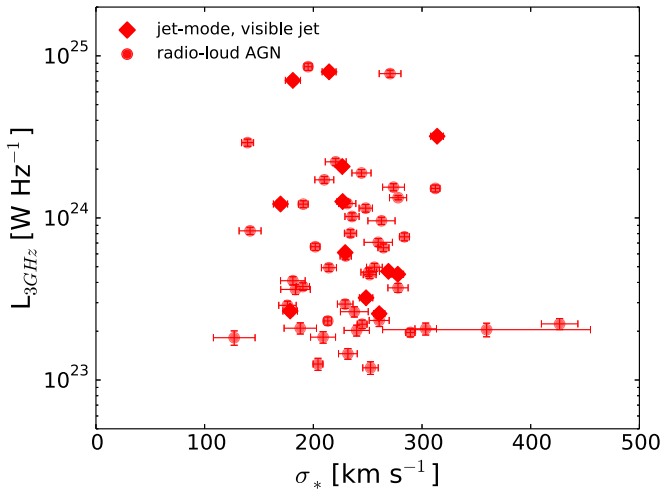
Figure 6. The 3 GHz luminosity as a function of the stellar velocity dispersion σ_* for the LEGA-C+VLA cross-matched sample of galaxies.

galaxies with $\sigma_* \gtrsim 200\,\mathrm{km\,s^{-1}}$ have jet-mode AGNs, reaching 20%–30% at $\sigma_* \sim 300\,\mathrm{km\,s^{-1}}$. This behavior is only weakly dependent on star formation activity if at all, which suggests that jet-mode AGNs are not associated with quiescence, but rather with high σ_*. Below $\sigma_* = 175\,\mathrm{km\,s^{-1}}$, we find three jet-mode AGNs (one 100% and two 50% objects), whereas if the power-law trend seen at high σ_* were to continue to low σ_*, we would expect a total of 10 jet-mode AGNs in the three low-σ_* bins. The detection of only three jet-mode AGNs may suggest a threshold black hole mass of $\sim 10^8\,M_\odot$ for jet-mode AGNs, as inferred from the local black hole mass–σ_* relation (Gebhardt et al. 2003; Beifiori et al. 2012; van den Bosch 2016). We argue that this threshold is not artificially introduced by our radio luminosity limit, as there is virtually no correlation between σ_* and radio luminosity as shown in Figure 6.

Assuming that the jet-mode fraction of 10%–30% at high σ_* can be interpreted as a duty cycle, we convert these fractions into the period (or frequency) at which galaxies turn on a jet-mode AGN. To make the conversion of the fraction of jet-mode AGNs into the period, we need a lifetime of an AGN jet.

Examination of the jet structure morphology of the 12 objects in Figure 3 reveals that they are reminiscent of the classical Fanaroff-Riley I (FRI) type radio galaxy (Fanaroff & Riley 1974; Ledlow & Owen 1996). It has been argued that lifetimes evolve with redshift (Athreya & Kapahi 1998), but among our radio galaxies that are detected in the pre-existing 1.4 GHz VLA data (Schinnerer et al. 2010), we find that the spectral slopes, and therefore presumably the ages, are similar to local counterparts (see Table 1). The typical spectral slopes of local counterparts range between $-1.3 < \alpha < -0.5$ with the average spectral slope being -0.8 (Condon 1992). Parma et al. (1998) find a correlation for FRI radio galaxies between the linear size of the jet and the synchrotron age of the jet as traced by the spectral slope, implying typical jet ages of about 100 Myr with an uncertainty of at most a factor 2. We therefore assume a lifetime of $2 \times 100\,\mathrm{Myr}$ and show the resulting periods in Figure 5 on the left. We conclude that galaxies turn on a jet-mode AGN about once every Gyr, provided that it has a stellar velocity dispersion in excess of $\sigma_* = 175\,\mathrm{km\,s^{-1}}$, corresponding with a black hole mass of $10^8\,M_\odot$. Remarkably, this is the same black hole mass threshold that has been shown to separate quiescent and star-forming galaxies in the local universe (Terrazas et al. 2016).

3.2. Stellar Populations of Galaxies with Radio-loud AGNs

Our $z \sim 1$ radio AGN typically live in red, quiescent galaxies (Figure 7) as was shown before by Smolčić et al. (2009), Simpson et al. (2013), and Rees et al. (2016).

With the LEGA-C spectra, we can examine, for the first time, the detailed stellar population properties of $z \sim 1$ radio galaxies. Figure 8 shows the Balmer absorption line index Hδ as a function of the 4000 Å break $D_n(4000)$ (Bruzual et al. 1983; Balogh et al. 1999; Kauffmann et al. 2003b; P.-F. Wu et al. 2017, in preparation). Both of these parameters trace the recent star formation activity within the galaxy. This shows that the jet-mode AGNs have a strong $D_n(4000)$ and weak Balmer absorption, which implies that these galaxies have been quiescent for more than a Gyr (Bruzual & Charlot 2003). That is, the observed AGNs with a lifetime of $\sim 100\,\mathrm{Myr}$ are not immediately responsible for the quenching
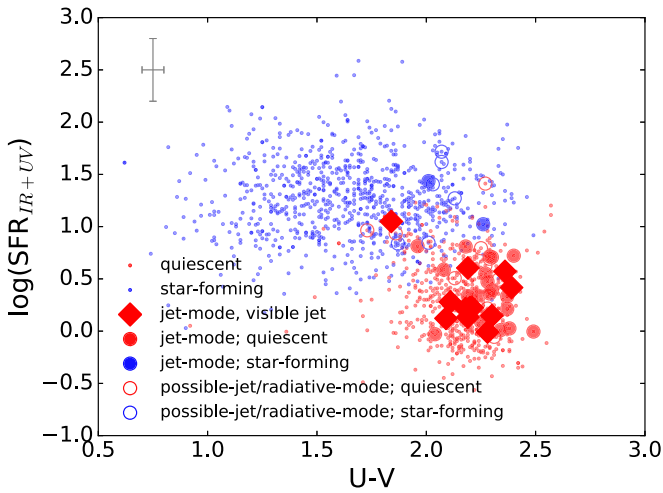
Figure 7. SFR_{UV+IR} as a function of the rest-frame UV color. The symbols are described in Figure 5. Jet-mode AGNs reside in red, quiescent galaxies, as had been demonstrated before.
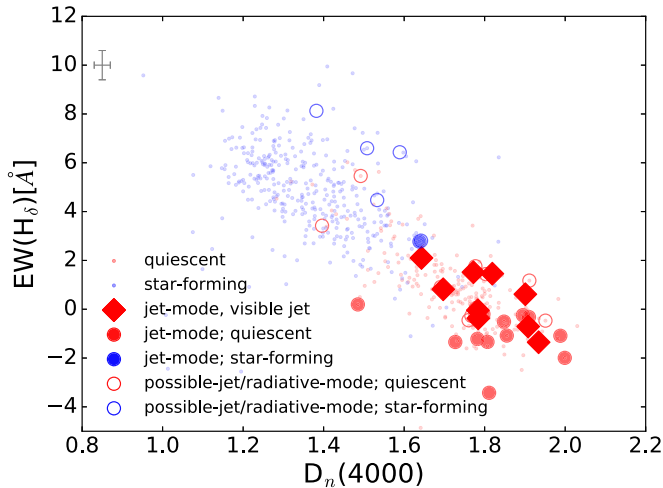

Figure 8. Balmer absorption line index Hδ as a function of the 4000 Å break $D_n(4000)$. The symbols are explained in Figure 5. Jet-mode AGNs occur in galaxies with old stellar populations, with little star formation activity for at least a Gyr.

of recent star formation. However, they may play a crucial role in maintaining quiescence, at least over the past 7 Gyr.

4. Conclusions

Maintenance-mode feedback from central BHs is a key element of all galaxy formation models in a cosmological context. Jet-mode AGNs are the physical manifestation of this concept, and a minimum requirement for the model in general is that jet-mode AGNs frequently occur in galaxies devoid of significant levels of star formation. This hypothesis has thus far only been tested directly in the present-day universe, but in this paper we investigate whether jet-mode galaxies at $z \sim 1$ have been quiescent for an extended period of time.

We select the radio-loud subset of galaxies in the LEGA-C spectroscopic survey sample by matching against the newly acquired VLA 3 GHz data set (Smolcic et al. 2017). We identify 58 radio-loud galaxies, most of which ($\sim$60%) are confirmed to be low-excitation radio AGNs. Most radio sources appear point-like, but 12 sources show clear jet-like morphologies and are classified as FRI types.

The galaxies that host these jet-mode AGNs have high stellar velocity dispersions of $\sigma_* > 175$ km s^{-1}, translating into a black hole mass threshold of $\sim 10^8 M_\odot$ for jet-mode AGNs, low specific star formation rates ($<10^{-1}$ Gyr^{-1}), and high stellar masses ($>10^{11} M_\odot$). The fraction of jet-mode AGNs is $\sim$30% among galaxies with the highest stellar masses $\gtrsim 10^{11} M_\odot$. Furthermore, strong 4000 Å breaks and weak Balmer absorption lines imply that these galaxies have been devoid of significant star formation activity for more than $\sim$1 Gyr. Assuming the jet-mode AGNs share similar physical properties in a certain mass bin, and considering their lifetime, we infer that every massive, quiescent galaxy at $z \sim 1$ will switch on a jet-mode AGN about once every Gyr.

Our findings put the conclusions by Best et al. (2014) on firmer footing, who statistically link the quiescent and radio-loud populations by comparing the evolution of their respective luminosity functions out to $z \sim 1$. It therefore seems increasingly plausible that radio AGNs play a crucial role across cosmic time in keeping the halo gas around massive galaxies hot, preventing further star formation.

ORCID iDs

Ivana Barišić ⊙ https://orcid.org/0000-0001-6371-6274
Arjen van der Wel ⊙ https://orcid.org/0000-0002-5027-0135
Rachel Bezanson ⊙ https://orcid.org/0000-0001-5063-8254
Camilla Pacifici ⊙ https://orcid.org/0000-0003-4196-0617
Marijn Franx ⊙ https://orcid.org/0000-0002-8871-3026
Eric F. Bell ⊙ https://orcid.org/0000-0002-5564-9873
Gabriel Brammer ⊙ https://orcid.org/0000-0003-2680-005X
Priscilla Chauké ⊙ https://orcid.org/0000-0002-1442-984X
Pieter G. van Dokkum ⊙ https://orcid.org/0000-0002-8282-9888
Anna Gallazzi ⊙ https://orcid.org/0000-0002-9656-1800
Ivo Labbé ⊙ https://orcid.org/0000-0002-2057-5376
Michael V. Maseda ⊙ https://orcid.org/0000-0003-0695-4414
Adam Muzzin ⊙ https://orcid.org/0000-0002-9330-9108
David Sobral ⊙ https://orcid.org/0000-0001-8823-4845
Caroline Straatman ⊙ https://orcid.org/0000-0001-5937-4590
Po-Feng Wu ⊙ https://orcid.org/0000-0002-9665-0440

References

Athreya, R. M., & Kapahi, V. K. 1998, JApA, 19, 63
Balogh, M. L., Morris, S. L., Yee, H., Carlberg, R., & Ellingson, E. 1999, ApJ, 527, 54
Beifiori, A., Courteau, S., Corsini, E., & Zhu, Y. 2012, MNRAS, 419, 2497
Bell, E. F. 2003, ApJ, 586, 794
Bell, E. F., Wolf, C., Meisenheimer, K., et al. 2004, ApJ, 608, 752
Best, P., Kauffmann, G., Heckman, T., et al. 2005, MNRAS, 362, 25
Best, P., Ker, L., Simpson, C., Rigby, E., & Sabater, J. 2014, MNRAS, 445, 955
Blanton, E. L., Sarazin, C. L., McNamara, B. R., & Wise, M. W. 2001, ApJL, 558, L15
Bower, R., Benson, A., Malbon, R., et al. 2006, MNRAS, 370, 645

Bruzual, A., et al. 1983, ApJ, 273, 105
Bruzual, G., & Charlot, S. 2003, MNRAS, 344, 1000
Calhau, J., Sobral, D., Stroe, A., et al. 2017, MNRAS, 464, 303
Calzetti, D., Armus, L., Bohlin, R. C., et al. 2000, ApJ, 533, 682
Chabrier, G. 2003, PASP, 115, 763
Condon, J. 1992, ARA&A, 30, 575
Croton, D. J., Springel, V., White, S. D., et al. 2006, MNRAS, 365, 11
De Breuck, C., Van Breugel, W., Stanford, S., et al. 2002, AJ, 123, 637
De Lucia, G., & Blaizot, J. 2007, MNRAS, 375, 2
Delhaize, J., Smolcic, V., Delvecchio, I., et al. 2017, A&A, 602, A4
Di Matteo, T., Springel, V., & Hernquist, L. 2005, Natur, 433, 604
Donoso, E., Best, P., & Kauffmann, G. 2009, MNRAS, 392, 617
Faber, S., Willmer, C., Wolf, C., et al. 2007, ApJ, 665, 265
Fanaroff, B., & Riley, J. 1974, MNRAS, 167, 31P
Gebhardt, K., Richstone, D., Tremaine, S., et al. 2003, ApJ, 583, 92
Heckman, T. M., & Best, P. N. 2014, ARA&A, 52, 589
Hine, R., & Longair, M. 1979, MNRAS, 188, 111
Hopkins, P. F., Quataert, E., & Murray, N. 2012, MNRAS, 421, 3522
Kauffmann, G., Heckman, T. M., Tremonti, C., et al. 2003a, MNRAS, 346, 1055
Kauffmann, G., Heckman, T. M., White, S. D., et al. 2003b, MNRAS, 341, 33
Laing, R. 1994, in ASP Conf. Ser. 54, The First Stromlo Symposium: The
    Physics of Active Galaxies, ed. G. V. Bicknell, M. A. Dopita, & P. J. Quinn
    (San Francisco, CA: ASP), 227
Ledlow, M. J., & Owen, F. N. 1996, in IAU Symp. 175, Extragalactic Radio
    Sources, ed. R. Ekers, C. Fanti, & L. Padrielli (Cambridge: Cambridge
    Univ. Press), 238
LeFevre, O., Saïsse, M., Mancini, D., et al. 2003, Proc. SPIE, 4841, 1670

Magnelli, B., Ivison, R., Lutz, D., et al. 2015, A&A, 573, A45
Matthews, T. A., Morgan, W. W., & Schmidt, M. 1964, ApJ, 140, 35
McNamara, B., & Nulsen, P. 2007, ARA&A, 45, 117
Muzzin, A., Marchesini, D., Stefanon, M., et al. 2013, ApJS, 206, 8
Parma, P., Murgia, M., Morganti, R., et al. 1998, arXiv:astro-ph/9812413
Rees, G., Spitler, L., Norris, R., et al. 2016, MNRAS, 455, 2731
Schaye, J., Crain, R. A., Bower, R. G., et al. 2015, MNRAS, 446, 521
Schinnerer, E., Sargent, M., Bondi, M., et al. 2010, ApJS, 188, 384
Scoville, N., Aussel, H., Brusa, M., et al. 2007, ApJS, 172, 1
Shakura, N. I., & Sunyaev, R. A. 1973, A&A, 24, 337
Simpson, C., Westoby, P., Arumugam, V., et al. 2013, MNRAS, 433, 2647
Smolcic, V., Novak, M., Bondi, M., et al. 2017, A&A, 602, A1
Smolčić, V., Zamorani, G., Schinnerer, E., et al. 2009, ApJ, 696, 24
Terrazas, B. A., Bell, E. F., Henriques, B. M., & White, S. D. 2016, MNRAS,
    459, 1929
van den Bosch, R. C. 2016, ApJ, 831, 134
van der Wel, A., Noeske, K., Bezanson, R., et al. 2016, ApJS, 223, 29
Vogelsberger, M., Genel, S., Springel, V., et al. 2014, MNRAS, 444, 1518
Werner, N., Allen, S., & Simionescu, A. 2012, MNRAS, 425, 2731
Werner, N., Oonk, J., Sun, M., et al. 2014, MNRAS, 439, 2291
Whitaker, K. E., Van Dokkum, P. G., Brammer, G., & Franx, M. 2012, ApJL,
    754, L29
White, S. D., & Frenk, C. S. 1991, ApJ, 379, 52
White, S. D., & Rees, M. J. 1978, MNRAS, 183, 341
Williams, W., & Röttgering, H. 2015, MNRAS, 450, 1538
Willott, C. J., Rawlings, S., Jarvis, M. J., & Blundell, K. M. 2003, MNRAS,
    339, 173